

THERMOELECTRIC PROPERTIES MEASUREMENT FOR TUNGSTEN DISELENIDE SINGLE CRYSTAL

¹Kaushik Patel* and ²C. A. Patel

¹*Microbiology Department, Gujarat Vidyapith, Ahmedabad, Gujarat*

²*Shri U P Arts, Smt M G Panchal Science & Shri V L Shah Commerce College, Pilvai, Gujarat*

**Author for Correspondence: krpatel@gujaratvidyapith.org*

ABSTRACT

The directional anisotropy of WSe₂ crystals results in varied thermoelectric behavior depending on the crystallographic orientation, with in-plane transport typically outperforming out-of-plane transport. Temperature-dependent studies indicate a maximum figure of merit (ZT) at intermediate temperature ranges, pointing to promising use in waste heat recovery technologies. Enhancing the thermoelectric efficiency of WSe₂ materials may be possible through approaches such as elemental doping, nanoscale structuring, or forming heterostructures with other two-dimensional materials.

INTRODUCTION

Thermoelectric materials hold great promise for high-temperature power generation applications, especially in harnessing waste heat and supplying onboard power for deep-space missions. These materials can efficiently convert heat directly into electrical energy, given a significant temperature gradient and a high thermoelectric figure of merit (ZT).

In the last ten years, there has been a worldwide initiative to identify new materials with improved ZT values and to boost the thermoelectric properties of existing substances. Successfully developing these materials is anticipated to pave the way for new applications of thermoelectric devices and associated technologies, employing both bulk crystals and thin films. Nonetheless, enhancing the performance of thermoelectric materials necessitates a thorough understanding of the factors that affect their properties.

Zhang, W. investigates the electronic characteristics of WSe₂, which are vital for comprehending its thermoelectric capabilities [1]. Bhaskar studied the thermoelectric properties of transition metal dichalcogenides, including WSe₂, highlighting their potential in energy-related applications [2]. Lee concentrates on the thermal characteristics of WSe₂, a crucial factor in assessing thermoelectric efficiency [3]. Shi et al. specifically examined the anisotropic thermoelectric properties of WSe₂, which are closely related to the aims of this study [4]. Furthermore, this review underscores significant progress in thermoelectric material research, providing essential context for the development and enhancement of materials like WSe₂ for energy conversion purposes [5].

MATERIALS AND METHODS

To achieve precise thermopower measurements, it is essential to prepare samples meticulously and establish clear thermal conditions. Typically, there is a lack of detailed information regarding the measurement process and setup. This study outlines the creation of an experimental setup designed for both single crystals and polycrystals. This setup facilitates the measurement of thermopower in single crystals and bulk materials of varying sizes, with temperatures ranging from 300 K to 800 K. Figure 1 illustrates a diagram of the apparatus used for measuring the high-temperature Seebeck coefficient. The setup includes a well-insulated 250 W cylindrical heater. For mounting samples, two copper rods with flat plates at the ends are inserted into two cylindrical heaters. At the top, a sample mounting stage is formed by two copper plates separated by about 1–2 mm.

In this setup, both heaters are simultaneously powered by two separate power sources, which are managed by a Eurotherm 2604 temperature controller. This controller adjusts and maintains the operating temperature within ± 0.5 K, up to a maximum of 800 K. For measuring temperature, two K-type chromal-alumel thermocouples were employed. These thermocouples are known for their stability and resistance to oxidation at high temperatures. The temperature sensors used were K-type chromal-alumel thermocouples with diameters of either 0.01 in or 0.005 in. Their calibration data is dependable [6] and consistent, and the

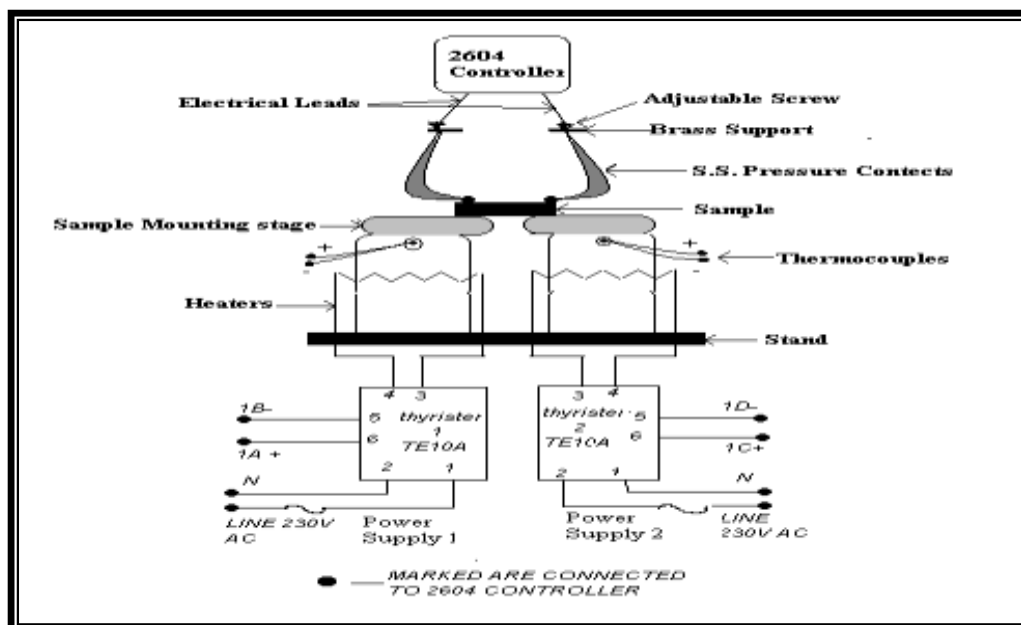


Figure 1: Block diagram and Experimental setup for thermopower measurement

thermocouple signal can be directly converted into a temperature reading with a precision of $0.001\text{ }^{\circ}\text{C}$ using the Eurotherm 2604 multipurpose controller. This controller is linked to a computer via MODBUS and manages both heaters.



Figure 2: Photograph of complete system

Complete Experimental Setup

Once the connections for the thyristors, heaters, and controller are established and the sample is secured, the entire setup is placed inside a vacuum chamber at a pressure of 10^{-3} Torr to minimize heat loss. A

preliminary heating process is conducted to facilitate degassing. The heater temperatures are adjusted within the desired range using a controller to ascertain the PID values, with a gradual heating rate of 1 °C per minute. The wires from the probes are shielded, and identical metal wires are used for both voltage leads and thermocouples, which are routed out of the vacuum chamber through a specially designed feed-through to prevent any artifacts from dissimilar junctions. Figure 2 displays the block diagram and photograph of the complete experimental setup.

To measure TEP, a sample of at least $3 \times 3 \text{ mm}^2$ is needed. First, the sample-mounting stage was cleaned with acetone. Then, the crystals were placed on copper plates. The sample ends were connected to electrical leads using stainless steel pressure contacts, adjusted with a screw. Measurements were taken between 300 K and 673 K. The temperature difference (ΔT) between the sample ends was kept between 5 and 10 K. A controller, linked to a computer, regulated the heater's current to maintain the desired ΔT . When an emf was generated for a specific temperature gradient, the controller detected it. The computer recorded the Seebeck coefficient ($S = \Delta V / \Delta T$) after ΔT was reached, with a three-minute delay for stable conditions. The hot probe was connected to the controller's negative terminal, and the cold probe to the positive terminal for thermo-emf measurements. N-type samples showed a negative Seebeck voltage, V. During measurement, an S→T curve was displayed on the computer, along with the latest data (S, T) with a 1 μV resolution. Data could be saved using the software's data-logging feature. The S-T curve was shown by the software's OPC Scope.

RESULTS AND DISCUSSION

The aim of the present work is to investigate the thermoelectric properties of a WSe₂ semiconductor single crystal, bearing in mind that information on the important thermoelectric parameters is required for assessing the applicability of semiconductor materials. The electrical properties were measured by measuring the Hall coefficient, resistivity, and thermoelectric power at different temperatures. The effective masses of the charge carriers were estimated using the relationship between the thermoelectric power (TEP) and carrier concentration. The thermoelectric effect is one of the most popular laboratory methods for measuring the electrical properties of semiconductors, such as the Fermi energy, carrier concentration, density of states, and effective mass of carriers. The thermoelectric effect offers a distinctive advantage over other methods because the measured thermoelectric voltage is directly related to the carrier concentration, which simplifies the thermoelectric measurement, even for low-mobility materials [7, 8]. Thermoelectric measurements are therefore frequently employed in the study of semiconductors as an independent method for determining the sign of charge carriers, effective density of states, position of the Fermi level in semiconductors [9-11], effective mass of the carriers, and scattering mechanism.

To gain a better understanding of the equipment, measurement methods, and data analysis, various TMDC single crystals were utilized. Transition metal dichalcogenides, which are composed of multiple compounds, are known for their significant thermoelectric properties [10,12-13]. They also exhibit anisotropic electrical characteristics both along and perpendicular to the basal planes. This is due to their layered M–X–M structure, where metal atoms (M) are positioned on either side of chalcogenide atoms. This results in a layered M – X – M...M – X – M...M – X – M structure with weak van der Waals forces between the M – X – M layers, while strong covalent bonds exist within each M – X – M layer. As a result, they can be easily cleaved along the c-axis. Numerous research papers and review articles [14] discuss the various properties of this group of TMDC compounds. In this study, several samples of WSe₂ single crystals were chosen to investigate their thermoelectric properties. Given the significance of Tungsten Diselenide (WSe₂) and thermoelectric materials, an in-depth examination of the thermoelectric properties of WSe₂ was conducted. These crystals were grown using the DVT technique [15, 16] and appeared as thin platelets with an opaque look and perfectly shiny surfaces. Thermoelectric power measurements were performed using the previously described experimental setup. Multiple experimental measurements were conducted on each sample, and the results were highly consistent. Typical observations of TEP measurements on the crystals, as mentioned earlier, were recorded for two different temperature gradients $\Delta T = 5 \text{ K}$ between heaters 1 and 2 of the apparatus. Typical observations for the crystals indicate that the WSe₂ crystals exhibit p-type conductivity. Figure 3 provides a graphical representation of the emf as a function of temperature for the WSe₂ crystals.

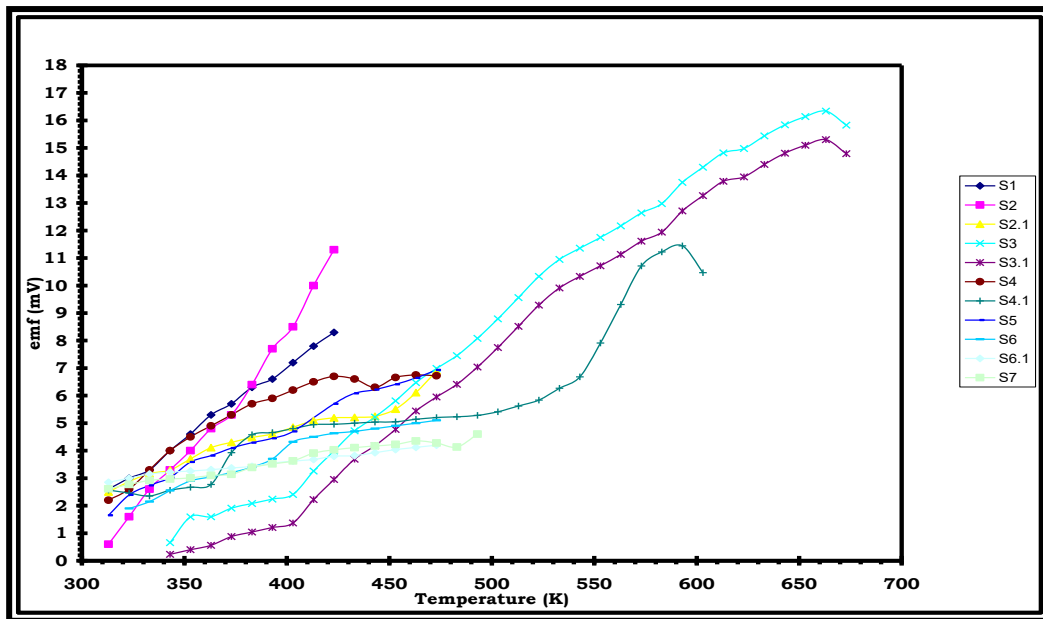


Figure 3: Thermo emf variation of WSe₂ crystal as a function of temperature ($\Delta T = 5$ K).

In this context, it is evident that the emf sign for the WSe₂ crystals is positive. The positive terminal of the voltmeter was connected to the cold probe, while the negative terminal was connected to the hot probe. Consequently, in n-type crystals, electrons near the hot probe gain additional thermal energy, resulting in a random velocity that exceeds that of electrons entering the hot region. This leads to a net transport of electrons toward the cooler areas of the specimen, causing the galvanometer to indicate the polarity of the hot probe. Conversely, for a p-type WSe₂ crystal, the opposite reasoning applies. Thus, p-type and n-type materials can be distinguished by the sign of the emf. Figure 4 illustrates the variation of thermoelectric power S of WSe₂ as a function of temperature, ranging from 300 K to 673 K, with $\Delta T = 5$ K.

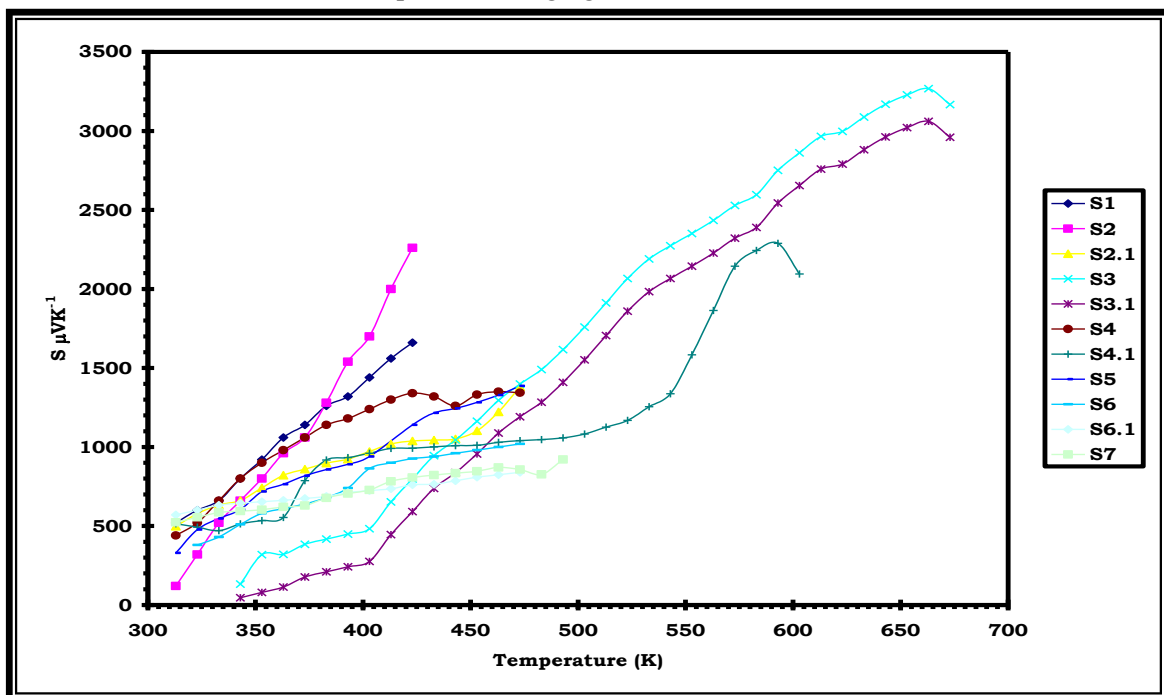


Figure 4: Variation of thermoelectric power S of WSe₂ single crystal

The above figures show that the value of “S” increases steadily with an increase in temperature, thus confirming the typical semiconducting behavior of different samples of WSe₂ [17]. This increasing trend of TEP with increasing temperature resembles that reported by Hicks [9] for WSe₂ in a similar temperature range. Figure 5 shows the variation in the thermoelectric power with the inverse of the temperature for the WSe₂ single crystals.

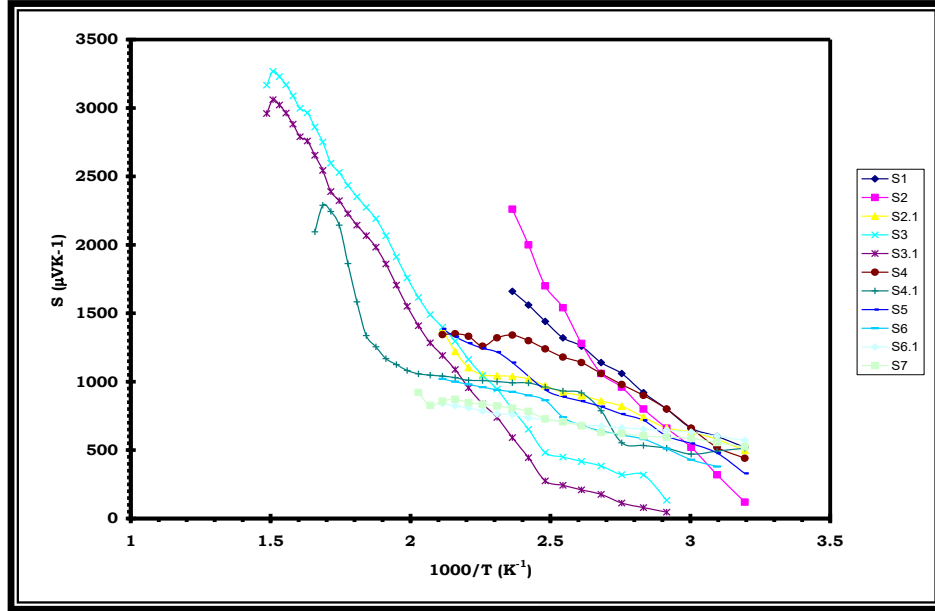


Figure 5: Variation of thermoelectric power S of WSe₂ single crystal as an inverse of temperature.

According to Hicks [9] and Rahman and Ashraf [18], a straightforward relationship can be derived for p-type non-degenerate semiconductors, which directly links the Seebeck coefficient to the carrier concentration ‘p’ [19].

$$S = \left[\frac{k}{e} \right] \left[A + \left\{ \frac{\ln 2 (2\pi m_h^* kT)^{3/2}}{ph^3} \right\} \right] \quad (1)$$

semiconductors, which directly links the Seebeck coefficient to the carrier concentration ‘p’ [19]. In this expression, k represents the Boltzmann constant, e is the electronic charge, h denotes the Planck constant, m_h^* is the effective mass of the charge carrier, T stands for temperature, and A is the scattering coefficient. The value of A is associated with the scattering mechanism and is related to the scattering parameter ‘s’ by the relation (2).

$$A = \left(\frac{5}{2} - s \right) \quad (2)$$

It is well established [17, 20-22] that in non-degenerate semiconductor materials, carriers are scattered in three distinct ways: (i) by ionized impurities (or defects), (ii) by acoustic phonons, or (iii) by optical phonons. When scattering occurs due to ionized impurities or defects, the mobility of the charge carriers increases with rising temperature. To examine the temperature dependence of the thermoelectric power S of a non-degenerate semiconductor, the expression provided by Mohanchandra and Uchil [8], Goldsmid H. J. [23], and Kwok [19] is used. This non-degenerate [21, 24-26]

$$S = -\frac{k}{e} \left[A + \frac{E_F}{kT} \right] \quad (3)$$

In Equation 3, the scattering coefficient A ranges from 0 to 4, contingent on the scattering process as previously mentioned; s represents the scattering parameter, and E_F denotes the distance between the Fermi level and the top of the valence band. By utilizing the values of A and the carrier concentration ' p ' obtained from room temperature Hall effect measurements, along with the ' S ' values from TEP measurements, the effective mass of charge carriers can be readily calculated using equation 1. The results are presented in Table 1. It is widely recognized that the carrier concentration in a crystal is primarily influenced by E_F . Within a narrow temperature range, E_F can be assumed to remain relatively stable; therefore, equations 1 and 3 imply that plotting TEP against the inverse of temperature (T^{-1}) should yield a straight line [27]. The slope of this line is recorded, and with the help of Equations 2 and 4, the Fermi energy E_F [27] can be calculated. In Table 1, the values of carrier concentration (measured using room-temperature Hall effect measurements), Fermi energy (from the slope of the thermopower vs. inverse of temperature), and scattering parameter' (from the intercept of the straight line on the y-axis of the thermopower) are shown for the WSe_2 crystals.

Table 1: Carrier Concentration, Fermi Energy, Effective Density of State, Effective Mass, Scattering Parameter of WSe_2 .

Crystals	Sample No.	Carrier concentration p (cm^{-3})	Fermi energy E_F (eV)	Effective Density of State N (m^{-3})	Effective Mass M_h^* (Kg)	m_h^*/m_h	Scattering Parameter s
WSe_2 $\Delta T = 5^\circ K$	1	9.110×10^{18}	0.0530	9.129×10^{24}	9.129×10^{-31}	1.02	2.48
	2	4.420×10^{18}	0.0924	4.436×10^{24}	5.799×10^{-31}	0.64	2.47
	2.1	4.420×10^{18}	0.0228	4.424×10^{24}	5.788×10^{-31}	0.64	2.49
	3	6.670×10^{18}	0.0521	6.683×10^{24}	7.600×10^{-31}	0.83	2.48
	3.1	6.670×10^{18}	0.0519	6.683×10^{24}	7.600×10^{-31}	0.83	2.48
	4	6.023×10^{18}	0.0278	6.029×10^{24}	7.101×10^{-31}	0.78	2.49
	4.1	6.023×10^{18}	0.0272	9.121×10^{24}	7.101×10^{-31}	0.78	2.49
	5	9.110×10^{18}	0.0315	9.121×10^{25}	4.265×10^{-30}	4.68	2.49
	6	1.120×10^{18}	0.0222	1.121×10^{24}	2.339×10^{-31}	0.26	2.49
	6.1	1.120×10^{18}	0.0078	1.120×10^{24}	2.338×10^{-31}	0.26	2.49
	7	9.110×10^{17}	0.0108	9.114×10^{23}	2.040×10^{-31}	0.22	2.49

As shown in Table 1, the scattering parameter ' s ' is approximately 2.49 for all crystals, indicating defect scattering [17, 20]. The relatively stable value of E_F suggests that the carrier concentration p does not significantly vary with temperature. Consequently, equation 4 can be rewritten as Table (4),

$$S = -\frac{k}{e} \left[A + \ln \left(\frac{N}{p} \right) \right] \quad (4)$$

where N represents the effective density of states (N_A for p-type and N_C for n-type materials) and is defined by the relation

$$N = 2 \left[\frac{2\pi m_h^* kT}{h^2} \right]^{\frac{3}{2}} \quad (5)$$

Here, m_h^* denotes the effective mass of charge carriers, and h is Planck's constant. By using the carrier concentration values obtained from Hall Effect measurements, the effective density of states N can be determined using the formula [20, 23, 28].

$$p = N \exp\left(-\frac{E_F}{kT}\right) \quad (6)$$

The effective density of states is found to be in the range of $10^{23} - 10^{24} \text{ m}^{-3}$ for the crystals being studied. By substituting the effective density of states values into equation 5, the effective mass of holes m_h^* was calculated, and these results are presented in Table 1.

CONCLUSION

All observations in this study were made using an indigenously developed setup. The sign of thermoelectric power in semiconducting materials depends on whether the majority carriers are electrons or holes. The positive sign of thermoelectric power from WSe₂ single crystals indicates p-type conductivity. Moreover, in all the compounds studied, there was no change in the sign of the TEP with increasing temperature within the measurement range of this study. This suggests that the materials maintain their semiconducting nature across the entire temperature range. The nature of the samples supports the conclusions drawn from Hall Effect measurements. The scattering constants for WSe₂ crystals indicate that charge carrier scattering is dominated by defect concentration in these crystals. It is well known that these layered compounds grow through a screw dislocation mechanism with a hexagonal structure, leading to the incorporation of defects like stacking faults in the structure. The values of E_F in Table 1 represent the distance of the Fermi energy level from the top of the valence band [27, 29]. The effective mass of the carriers has been estimated from the TEP measurement using Equation 5, assuming defect scattering. The calculated values provide crucial insights into the electronic properties of these crystals, enabling a deeper understanding of their behavior in various applications. These parameters play a significant role in determining the material's conductivity, optical properties, and overall performance in electronic devices. Further analysis of these values could lead to the development of more efficient and tailored materials for specific technological applications.

REFERENCES

- [1] Caillat, T., Fleurial, J.-P., & Borshchevsky, A. (1997). *Preparation and thermoelectric properties of semiconducting skutterudites*. Journal of Physics and Chemistry of Solids, **58**(7), 1119–1125.
- [2] Rowe, D. M. (Ed.). (1995). *CRC Handbook of Thermoelectrics*. CRC Press, London & New York.
- [3] Rowe, D. M., & Bhandari, C. M. (1983). *Modern Thermoelectrics*. Holt, Saunders, London.
- [4] Hunter, R. A., Rittner, E. S., & Dupré, F. K. (1950). *Fermi levels in semiconductors*. Philips Research Reports, **5**, 188–198.
- [5] Fistul, V. I. (1969). *Heavily Doped Semiconductors*. Plenum Press, New York.
- [6] Zhou, Z., & Uher, C. (2005). *Automated system for measuring the Seebeck coefficient under large temperature gradients*. Review of Scientific Instruments, **76**, 023901.
- [7] Kwok, H. B., & Bube, R. H. (1973). *Electrical transport properties of compound semiconductors*. Journal of Applied Physics, **44**(1), 138–144.
- [8] Brixner, L. H. (1963). *Preparation and properties of semiconducting metal chalcogenides*. Journal of The Electrochemical Society, **110**, 289–294.
- [9] Hicks, W. T. (1964). *Electrical properties of semiconducting sulfides*. Journal of The Electrochemical Society, **111**, 1058–1063.
- [10] Gujarathi, D. N. (2004). *Studies on electrical and thermoelectric properties of chalcogenide materials*. Ph.D. Thesis, Sardar Patel University, Vallabh Vidyanagar, Gujarat, India.
- [11] Makhija, D., Patel, M., Jani, M. S., & Jakhmola, P. R. (2008). *Electrical and thermoelectric studies of chalcogenide compounds*. Journal of Pure and Applied Sciences (Prajna), **16**, 172–176.

- [12] Li, T., & Galli, G. (2007). *Electronic and thermal transport properties of thermoelectric materials from first principles*. The Journal of Physical Chemistry C, **111**, 16192–16196.
- [13] Sams, W., Russell, M., Bhattacharya, S., Lowhorn, N., Tritt, T. M., & Abbott, E. (2003). *Thermoelectric characterization of novel chalcogenide materials*. Bulletin of the South Carolina Academy of Science.
- [14] Wilson, J. A., & Yoffe, A. D. (1969). *The transition metal dichalcogenides: Optical, electrical and structural properties*. Advances in Physics, **18**, 193–335.
- [15] Sumesh, C. K. (2008). *Electrical and thermoelectric properties of layered chalcogenides*. Ph.D. Thesis, Sardar Patel University, Vallabh Vidyanagar, Gujarat, India.
- [16] Makhija, D. L. (2009). *Transport properties of chalcogenide semiconductor materials*. Ph.D. Thesis, Sardar Patel University, Vallabh Vidyanagar, Gujarat, India.
- [17] Solanki, G. K., Gujarathi, D. N., Deshpande, M. P., Laxminarayana, D., & Agarwal, M. K. (2008). *Electrical and thermoelectric properties of layered semiconducting crystals*. Crystal Research and Technology, **43**(2), 179–185.
- [18] Rahman, M. A., & Ashraf, I. M. (1998). *Electrical transport in semiconducting chalcogenide thin films*. Journal of Physics D: Applied Physics, **31**, 889–894.
- [19] Vora, M. M., & Vora, A. M. (2007). *Thermoelectric power studies of chalcogenide compounds*. Chalcogenide Letters, **4**, 77–82.
- [20] Perluzzo, G., Lakhani, A. A., & Jandl, S. (1980). *Electrical conductivity and thermopower of layered semiconductors*. Solid State Communications, **35**, 301–305.
- [21] Singh, J. P. (1995). *Electrical and dielectric properties of semiconducting materials*. Journal of Materials Science: Materials in Electronics, **2**, 105–110.
- [22] Zoater, M., Conan, A., Bonnet, A., & Ramout, D. (1984). *Transport properties of layered semiconductor crystals*. Physica Status Solidi (b), **124**, 403–410.
- [23] Goldsmid, H. J. (1950). *Applications of Thermoelectricity*. Methuen Monograph, London.
- [24] Lee, P. A., Said, G., Davis, R., & Lim, T. (1969). *Electron transport in layered semiconductors*. Journal of Physics and Chemistry of Solids, **30**, 2719–2725.
- [25] Lee, P. A., Said, G., Davis, R., & Lim, T. (1969). *Electrical conductivity anomalies in layered compounds*. Solid State Communications, **7**, 1359–1363.
- [26] Patel, S. G., Agarwal, M. K., Batra, N. M., & Lakshminarayana, D. (1998). *Thermoelectric power studies of chalcogenide crystals*. Bulletin of Materials Science, **21**, 213–218.
- [27] Zoater, M., Conan, A., & Delaunay, D. (1977). *Electrical transport in layered semiconducting materials*. Physica Status Solidi (a), **41**, 629–635.
- [28] Patel, J. B., Parmar, M. N., Deshpande, M. P., Solanki, G. K., & Agarwal, M. K. (2005). *Thermoelectric and electrical properties of layered chalcogenides*. Journal of Pure and Applied Physics, **43B**, 527–532.
- [29] Solanki, G. K., Vashi, M. N., Patel, Y. A., Unadkat, S., & Agarwal, M. K. (2008). *Thermoelectric transport properties of chalcogenide semiconductors*. Chalcogenide Letters, **5**, 39–44.